Int. J. Electrochem. Sci., 13 **(2018)** 3475 – 3485, doi: 10.20964/2018.04.18

International Journal of
ELECTROCHEMICAL
SCIENCE
www.electrochemsci.org

Comparing the Support Effects of Graphene Nanosheets (GNs) and N-doped GNs with Respect to Anti-Poisoning Performance of Pt Catalysts

Yujie Yang[1], *Jianshe Wang*[1,*], *Changhai Liu* [2,*], *Niancai Cheng*[3], *Xueliang Sun*[4]

[1] School of Chemical Engineering and Energy, Zhengzhou University, Zhengzhou, Henan, 450000, P. R. China
[2] School of Materials Science & Engineering, Jiangsu Collaborative Innovation Center of Photovoltaic Science and Engineering, Changzhou University, Changzhou, Jiangsu 213164, P.R. China
[3] School of Materials Science & Engineering, Fuzhou University, Fuzhou, Fujian, 350116, P. R. China
[4] Department of Mechanical and Materials Engineering, The University of Western Ontario, ON, N6A 5B9, Canada
[*]E-mail: wangjs07@zzu.edu.cn, liuch@cczu.edu.cn.

Received: 9 January 2018 / *Accepted:* 5 February 2018 / *Published:* 6 March 2018

It is of great significance to precisely evaluate the anti-poisoning performance (APP) of anode catalysts for development of direct liquids fuel cells. By controlloing the similarity of Pt deposited on graphene nanosheets (GNs) and N-dopped GNs (NGNs), Pt/GNs and Pt/NGNs were prepared as model catalysts for APP evaluation. Cyclic voltammograms (CVs) of Pt/GNs and Pt/NGNs for formate and methanol oxidation showed that the APP differences of two catalysts were hardly distinguished only from CVs because the activities of the two catalysts were similar. By further analyzing the i-t data, Pt/NGNs was proved to be evidently superior to Pt/GNs in terms of APP, verifying the necessity of APP analysis for comprehensive catalysts evaluation. Furthermore, by analyzing Raman spectra, CO stripping and X-ray photoelectron spectroscopy, stronger interaction between Pt and NGNs was shown to produce weaker adsorption of poisoning species on NGNs-supported Pt, which is benificial for enhancing APP of Pt/NGNs. We believe this understanding can shed light on future work toward rational supports engineering for APP improvement.

Keywords: Anti-poisoning performance; Pt catalysts; graphene; i-t measurement; formate oxidation

1. INTRODUCTION

As is well known, catalysts play decisive role in fuel cells development. Catalysts with superior activity, selectivity, stability and anti-poisoning performance (APP) are highly desirable [1-4]. To develop high-performance catalysts, a great deal of research have been conducted to investigate the

structure-performance relationship from the aspects of catalysts size [5, 6], morphology [7, 8], composition [9], crystalline structure [10] and catalysts supports [11-13]. Catalysts supports not only determine the dispersion and physical stability of catalysts, but also influence the activity and APP of supported catalysts through strong interactions between catalysts and supports [14-16]. Therefore, it is of vital significance to investigate the influence of supports for rationally designing and screening superior supports.

For direct liquids fuel cells (DLFCs), it is an urgent task to enhance the APP of anode catalysts because the poisoning of anode catalysts directly leads to inferior performance of DLFCs [17-19]. To improve the APP, standard methods for evaluating APP should be available for investigating the structure-APP relationship, which can then be used for improving catalysts. However, up to now, APP evaluation methods for formic acid [20], methanol [21] and ethanol oxidation catalysts [22] still need further normalization, and only limited researches have been conducted on the APP of formate oxidation catalysts [23, 24]. For example, evaluating APP based on ratio of forward currents (I_f) to backward currents (I_b) recorded from cyclic voltammograms (CVs), although widely used and sometimes consistent with APP [25-27], is still under debates [28-30]. Some APP comparison were conducted only based upon CVs without measuring corresponding i-t curves [31]. When evaluating APPs of several catalysts according to i-t curves, only ending currents were compared without considering the difference in initial activities or the decaying rates [15, 32, 33]. On the other hand, controlled comparison is necessary when studying the APPs varying with various parameters, especially when the differences in APP are not quite distinct. For example, when studying the support effects on APPs of Pt catalysts, Pt properties should be controlled to be unchanged while only changing the properties of supports [12, 34-36]. However, to our knowledge, precisely comparing catalysts APP based upon well-controlled preparation has not become a widely accepted prototype up to now.

Recently, we compared APP of Pt catalysts supported on carbon nanotubes (CNTs) and graphene for formate oxidation and found that graphene is more favorable for improving APP of Pt catalysts [37]. As a continuing work, in this study, graphene nanosheets (GNs) and N-doped GNs (NGNs) were used as supports for depositing well-controlled Pt particles. The two catalysts were found similar in activity for formate and methanol oxidation, indicating that the difference in GNs and NGNs is too trivial to be revealed. Fortunately, by comparing the two catalysts in terms of APP using our evaluation methods, we eventually demonstrated that NGNs are superior to GNs for improving APP of Pt catalysts, confirming the necessity of APP characterization for comprehensive catalysts evaluation. Furthermore, by ascribing this result to the stronger interaction between Pt and NGNs versus GNs, we demonstrated an efficient avenue for catalyst improvement through support engineering.

2. EXPERIMENTAL

2.1. Chemicals

$H_2PtCl_6 \cdot 6H_2O$, potassium formate (HCOOK) and other reagents were of analytical purity and used without further purification.

GNs were prepared through exfoliating graphite oxide via a thermal treatment at 1050 ^{o}C under Ar atmosphere. NGNs was obtained by further heating the GNs under high purity ammonia mixed with Ar at 900 ℃ [38].

2.2. Preparation of Pt catalysts supported on GNs and NGNs

Pt particles were first prepared in 50 mL ethylene glycol(EG) solution containing 170 mg NaOH and 55 mg $H_2PtCl_6 \cdot 6H_2O$ by microwave heating for 1 min. The obtained Pt nanoparticles in EG solution were equally divided into two parts. One part was added drop-wise into a beaker containing 40 mg GNs and another into a beaker containing 40 mg NGNs. After magnetic stirring for 3 h, each mixture was filtered, washed with de-ionized water, and dried for use. The obtained two sample was denoted as Pt/GNs and Pt/NGNs, the Pt content in which was determined using inductively coupled plasma (ICP) emission spectrometer to be 19.3 wt. % and 20.1 wt. %, respectively.

2.3. Physical characterization of Pt/GNs and Pt/NGNs

The X-ray diffraction (XRD) patterns of Pt/GNs and Pt/NGNs were recorded on a Rigaku X-ray diffractometer (X´Pert Pro, Panalytical Company, Netherlands) using Cu-Ka as radiation source. Diffraction data were collected with 2θ angels scanning from 10° to 85°.

The Raman spectra were performed from 500 to 2500 cm^{-1} at room temperature using a Roman spectrometer (DXR, USA) with a 532 nm Nd:YAG laser excitation source.

X-ray photoelectron spectra (XPS) were obtained using an Axis Ultra (Kratos Analytical, UK) XPS spectrometer equipped with an Al Kα source (1486.6 eV) in ultrahigh vacuum. The binding energies were referenced to the C1s line at 284.8 eV from adventitious carbon.

Transmission electron microscopy (TEM) images was observed on a FEI Talos F200X transmission electron microscope to determine the morphology of the catalysts. The corresponding size distribution histograms for each sample was obtained by measuring ~ 200 particles.

2.4.Electrochemical characterization of Pt/GNs and Pt/NGNs

Catalysts inks were first prepared for casting on a glassy carbon (GC, Φ=3 mm) electrode. Briefly, 2 mg of Pt/GNs or Pt/NGNs was dispersed in a solution (520 μL ethanol and 80 μL of 5 wt% Nafion) and ultrasonically blended for 30min. 15 μL of this suspension was dropped on the GC electrode and dried using an infrared lamp.

Electrochemical experiments were conducted using a three-electrode cell by a CHI electrochemical workstation (CHI 660B, Shanghai Chenhua Instrument CO., Ltd., China). GC electrode coated with catalysts was used as working electrode (WE). A Pt wire electrode and a saturated calomel electrode (SCE) electrode were used as counter electrode and reference electrode, respectively. Before each testing, the GC electrode was cleaned by polishing with 30~50 nm alumina power suspension followed by ultrasonic cleaning in de-ionized water. All potentials in this study were

referred to SCE, and all the electrochemical experiments were conducted at 25 °C in a N_2-saturated solution.

For each catalyst characterization, stable cyclic voltammograms (CVs) were first recorded by potential scanning at 50 mV s^{-1} in 1 M KOH solution. Then CVs for formate oxidation (or methanol oxidation) were recorded by starting from -0.9 V, followed by corresponding i-t measurement at -0.65 V for formate oxidation (or -0.3 V for methanol oxidation) for 2500 s. It deserves noting that each working electrode was preconditioned at 0.3 V for 3 s before recording the CVs or i-t data.

For CO stripping measurements, gaseous CO was bubbled into the electrolyte (1 M KOH) for 30 min adsorption onto the electrode while keeping the electrode potential at -0.9 V. Excess CO in solution was then purged out by gaseous nitrogen for another 30 min. Then two successive CVs for CO stripping were recorded at a rate of 20 mV s^{-1}.

3. RESULTS AND DISCUSSION

3.1.XRD, Raman and TEM results for Pt/GNs and Pt/NGNs

Fig. 1(a) shows the XRD patterns of Pt/GNs and Pt/NGNs. It can be seen that the overall profiles of the two patterns are quite similar. The peak at 26.4° and 39.6° can be ascribed to the carbon (002) and Pt(111) plane diffraction, respectively. The width of the two peaks at 39.6° is nearly identical, confirming the controlled similarity of Pt depositing on GNs and NGNs.

Raman spectra were collected to investigate the structural difference between Pt/GNs and Pt/NGNs, as shown in Fig. 2(b). Two characteristic peaks at ~1340 cm^{-1} and ~1580 cm^{-1} can be ascribed to the D band and G band, respectively [14, 31, 39]. It is well-accepted that the D band originates from the sp^3 hybridized carbon, i.e., disordered carbon while the G band is associated with the sp^2 hybridized carbon, i.e., graphitized carbon. The ratio of the D band intensity (I_D) to the G band intensity (I_G) can be used to reflect the degree of defect within a carbon material. The calculated values of I_D/I_G for Pt/GNs and Pt/NGNs were 1.09 and 1.40, respectively, indicating that NGNs possess higher degree of defects than GNs.

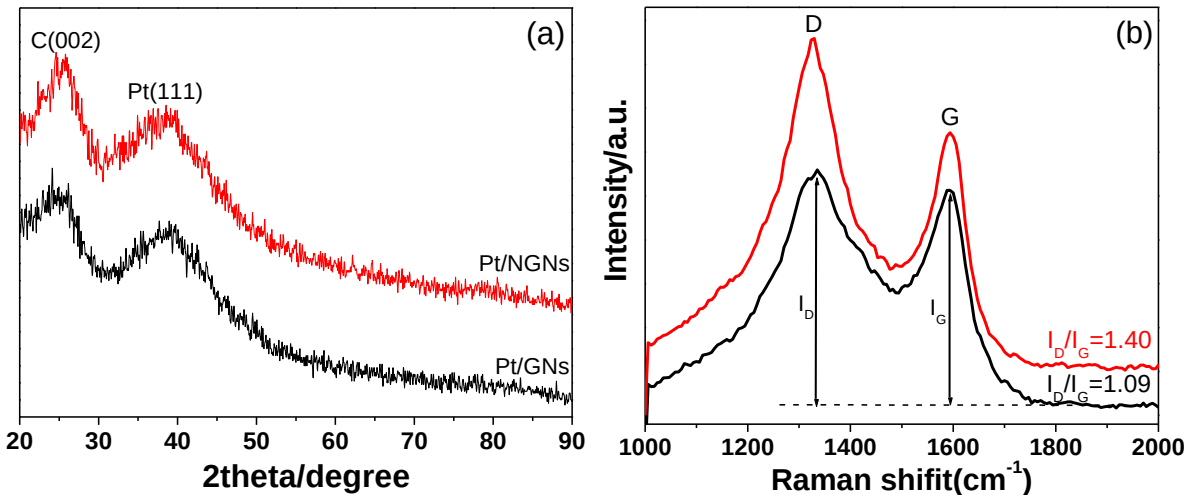

Figure 1. (a) XRD patterns and (b) Raman spectra of Pt/GNs (black line) and Pt/NGNs (red line).

The TEM graph and enlarged micrograph of Pt/GNs are shown in Fig. 2(a) and 2(b), and those for Pt/NGNs are shown in Fig. 2(c) and 2(d), respectively. It can be seen that Pt particles were homogeneously dispersed on GNs and NGNs with no evident agglomeration, thanks to the large surface area of graphene structures. By measuring sizes of ~200 Pt particles in Pt/GNs and Pt/NGNs, we presented corresponding size distribution histograms as inset in Fig. 2(b) and Fig. 2(d). It can be seen that the Pt size distribution for Pt/GNs and Pt/NGNs is quite similar and the average Pt size were identical, that is, nearly 2.0 nm. This result, in agreement with the XRD results, further verified the controlled similarity of Pt depositing on GNs and NGNs.

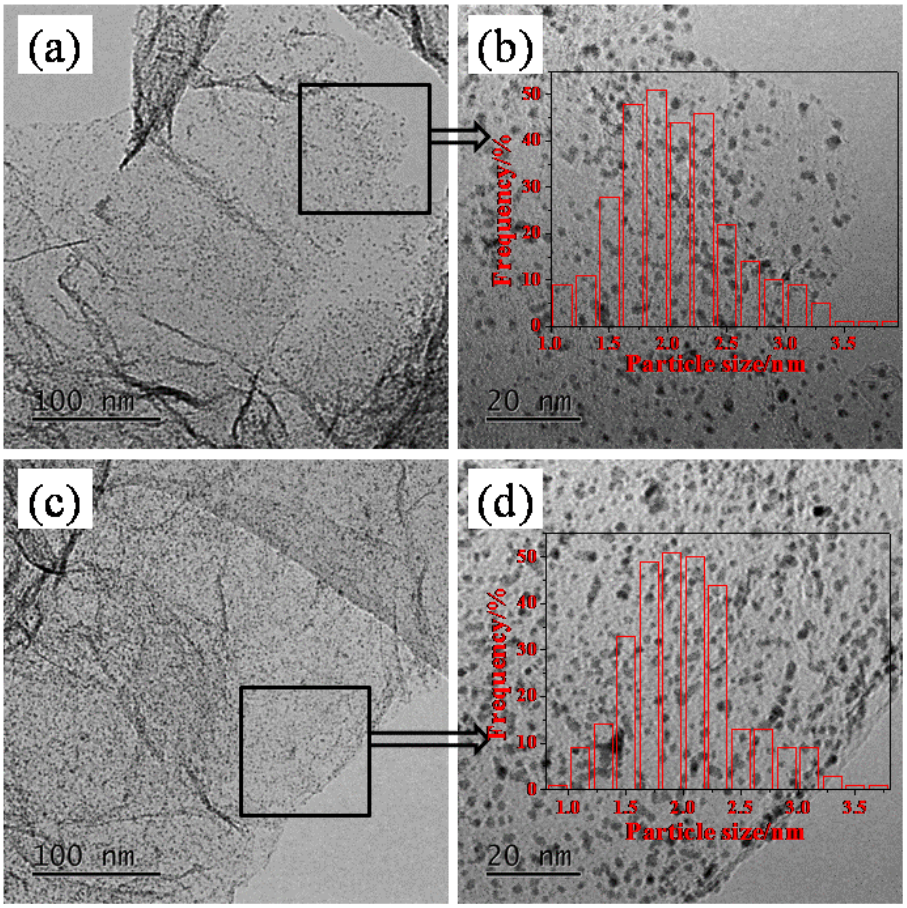

Figure 2. (a) TEM graph and (b) enlarged micrograph and size distribution histogram for Pt/GNs. (c) TEM graph and (d) enlarged micrograph and size distribution histogram for Pt/NGNs.

3.2.Electrochemical characterization of Pt/GNs and Pt/NGNs

For electrochemical characterization of Pt/GNs and Pt/NGNs, stable CVs was first obtained by cyclic voltammetry (CV) tests in 1 M KOH. Then after obtaining stable CVs in 1 M KOH + 1 M HCOOK solution, two cycles of CVs ranging from -0.9 V to 0.1 V were recorded at 50 mV s^{-1}, as shown in Fig. 3 (a). The CVs of Pt/GNs and Pt/NGNs in 1 M KOH solution were also recorded for reference (black lines). Following CV tests, corresponding i-t curves for Pt/GNs and Pt/NGNs were also recorded, as shown in Fig. 3(b).

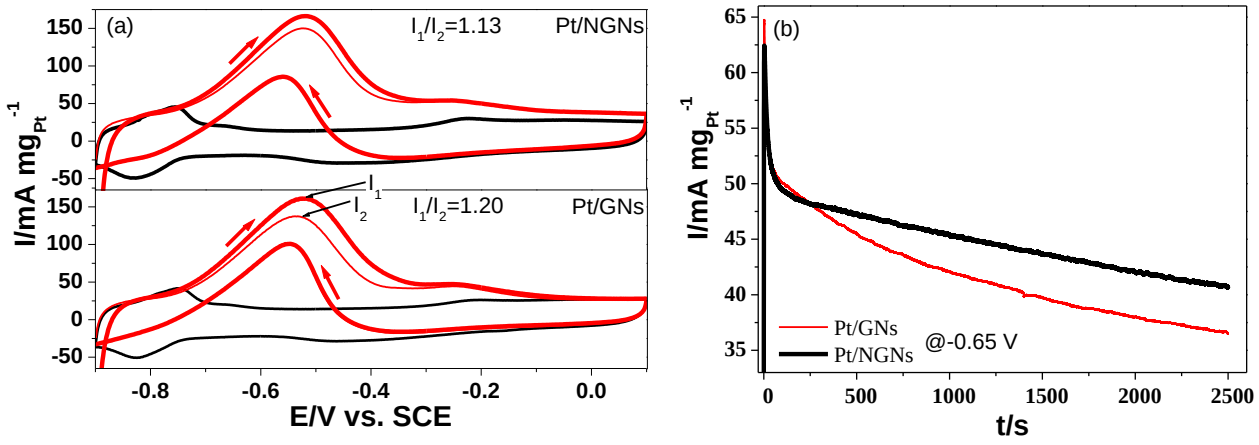

Figure 3. (a) CVs recorded in 1 M KOH + 1 M HCOOK for Pt/GNs and Pt/NGNs at 50 mV s^{-1} and (b) corresponding i-t curves recorded at -0.65 V. The red thick and thin lines in (a) show CVs of the first and second cycles. The black lines represent CVs recorded in 1 M KOH at 50 mV s^{-1}.

From CVs of Pt/GNs and Pt/NGNs with similar profiles, we can see that the values of forward peak currents for two catalysts are quite close, indicating that their activities are similar within the experimental error limit. However, when examining the peak currents decaying from the first to the second cycle of CVs, we can notice some difference for the two catalysts. Specifically, the extent of peak current decay for Pt/NGNs is smaller than that of Pt/GNs, as shown in Fig. 3(a). To understand this phenomena, it deserves explaining herein that the first cycle of CVs (red thick line) was recorded after preconditioning the electrode at 0.3 V for 3 s. By such doing, the poisoning species on Pt surface could be cleaned [23, 37]. For the second cycle (red thin line) without such a treatment, the poisoning species on Pt surface would suppress the formate oxidation, leading to a decrease in peak current. With this understanding, it is acceptable to evaluate the APPs of two catalysts using the ratio of I_1 to I_2 (I_1/I_2), where I_1 and I_2 means the peak currents recorded during the first and second cycles, respectively. Namely, a higher value of I_1/I_2 means a higher tendency to be poisoned. As shown in inset of Fig. 3(a), the value of I_1/I_2 for Pt/GNs (1.20) is higher than that of Pt/NGNs (1.13), indicating a higher APP for Pt/NGNs.

The difference in APPs for Pt/GNs and Pt/NGNs can be further seen from the corresponding i-t curves recorded at -0.65 V. The decaying rate of i-t curves for Pt/GNs is bigger than that of Pt/NGNs, and the ending current at 2500 s for the former is evidently lower than that of the latter, as shown in Fig. 3(b), indicating superior APP of Pt/NGNs to that of Pt/GNs. It deserves noting that we herein roughly evaluate the APPs of Pt/NGNs and Pt/GNs by directly comparing the ending current, without considering the initial CV currents at -0.65 V. This is because the corresponding cyclic voltammetry (CV) current (I_{CV}) for Pt/NGNs (72.4 mA mg_{Pt}^{-1}) are quite close to that of Pt/GNs (71.4 mA mg_{Pt}^{-1}). Strictly speaking, when the initial CV currents for two catalysts are different to a large extent, simply comparing the corresponding ending currents to evaluate the APPs is inaccurate or misleading. That is to say, the initial CV currents should be taken into consideration when analyzing i-t data for APP evaluation. Considering this, we proposed relative activity retention (RAR) [37] as an indicators for

APPs evaluation by combining i-t data (I_{i-t}) and CVs results (I_{CV}). Moreover, decaying rate (DR) [37] was also used for APPs analysis. The calculated results were shown in Table 1.

Table 1. APPs of Pt/GNs and Pt/NGNs analyzed from results in Figure 3

		500 s	1000 s	1500 s	2000 s	2500 s
I_{i-t}/mA mg_{Pt}^{-1}	Pt/GNs	45.5	42.1	39.8	38.0	36.5
	Pt/NGNs	47.3	45.3	43.7	42.1	40.7
RAR/%	Pt/GNs	63.7	59.0	55.7	53.2	51.1
	Pt/NGNs	65.3	62.6	60.3	58.1	56.2
DR/%	Pt/GNs	-	7.4	5.6	4.5	3.9
	Pt/NGNs	-	4.1	3.7	3.6	3.3

From Table 1 we can see that the RAR values of Pt/NGNs are all bigger than those of Pt/GNs during the whole time range, and the DR values of Pt/NGNs are all smaller than those of Pt/GNs, indicating the superior APP of Pt/NGNs to that of Pt/GNs. In fact, this difference is also true for the case of methanol oxidation. As shown in Fig. 4, the i-t currents (I_{i-t}) at -0.3 V for Pt/NGNs are all higher than those for Pt/GNs during the whole time range, undoubtedly indicating superior APP for Pt/NGNs to that of Pt/GNs, although their corresponding CV currents (I_{CV}) at -0.3 V (see the inset) are not largely different. The RAR and DR calculation (Table 2) further confirmed the superior APP of Pt/NGNs to that of Pt/GNs.

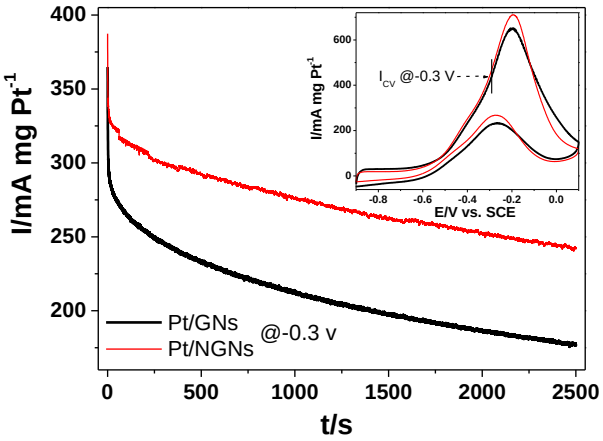

Figure 4. i-t curves recorded at -0.3 V in 1 M KOH + 1 M methanol for Pt/GNs and Pt/NGNs. The inset shows the corresponding CVs recorded at 50 mV s^{-1}.

Table 2. APPs of Pt/GNs and Pt/NGNs analyzed from results in Figure 4

		500 s	1000 s	1500 s	2000 s	2500 s
I_{i-t}/mA mg_{Pt}^{-1}	Pt/GNs	234	213	198	187	177
	Pt/NGNs	292	276	262	252	243
RAR/%	Pt/GNs	61.2	55.8	51.8	49.0	46.3
	Pt/NGNs	69.5	65.7	62.4	60.0	57.9
DR/%	Pt/GNs	-	9.0	7.0	5.5	5.3
	Pt/NGNs	-	5.5	5.1	3.8	3.6

On the other hand, since the ratio of forward currents to backward currents (I_f/I_b) has been widely employed for evaluating APP of catalysts [25-27, 29, 31, 32, 34], we herein also tried using this indicator for APP evaluation concerning methanol oxidation. The I_f/I_b values for Pt/GNs and Pt/NGNs are identical to be 2.45, failing to reflect the difference in APPs of the two catalysts. In fact, following the case of formate oxidation in Fig. 3(a) for APP evaluation, we also tried calculating the values of I_1/I_2 (data not shown) from corresponding CVs of Pt/GNs and Pt/NGNs, and found that there is no apparent decay from I_1 to I_2 for the case of methanol oxidation. These results reflected the necessity of i-t data for APP evaluation and confirmed the efficiency of our methods.

Since CO stripping has been widely used as a probing tool to investigate the APPs of catalysts [6, 8, 10, 11, 14, 20, 27, 29], CO stripping on Pt/GNs and Pt/NGNs were conducted in 1 M KOH solution (Fig. 5). It can be seen that the onset potential for CO oxidation on Pt/NGNs (-0.524 V) is evidently lower than that on Pt/GNs (-0.475 V), and the peak potential for Pt/NGNs is also lower than that for Pt/GNs, indicating facile CO stripping due to weaker strength of CO adsorption on Pt particles supported on NGNs than on GNs. Since Pt deposited on GNs and NGNs was well controlled with high similarity in size distribution and crystalline structure (see TEM and XRD results), the difference in APPs, including the CO stripping behavior, of Pt/GNs and Pt/NGNs can thus be ascribed to the different support effects of GNs vs. NGNs.

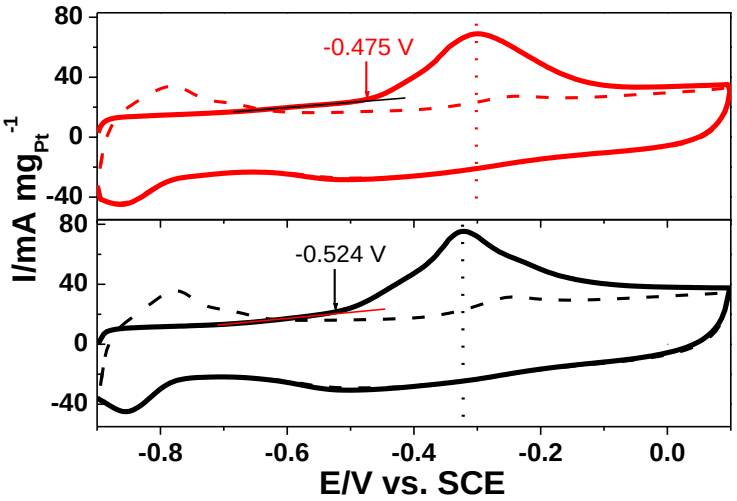

Figure 5. Curves for CO stripping on Pt/GNs (upper) and Pt/NGNs (lower) recorded at 20 mV s^{-1} in 1 M KOH solution.

To verify the different support effects of GNs and NGNs, X-ray photoelectron spectroscopy (XPS) was used to analyze the electronic structure of Pt in Pt/GNs and Pt/NGNs. From the full XPS spectra of Pt/GNs and Pt/NGNs in Fig. 6(a), N 1s peak at ~398.3 eV was detected on the surface of Pt/NGNs, indicating the successful doping of nitride element in NGNs. Fig. 6(b) show the XPS spectra of deconvoluted Pt 4f peaks for analyzing Pt state of Pt/GNs and Pt/NGNs. The more intense doublet (blue curves) located at 70.8 eV and 74.1 eV can be attributed to $4f_{7/2}$ and $4f_{5/2}$ of Pt^0. The higher energy signal peaks at 72.0 eV and 75.3 eV can be ascribed to Pt^{2+} species (e.g. PtO or $Pt(OH)_2$).

Notably, detectable positive shift of binding energy of Pt 4f was observed for Pt/NGNs at ~70.8 and ~72.0 eV in Fig. 6(b), confirming the stronger Pt-NGNs interaction in comparison with that of Pt-GNs.

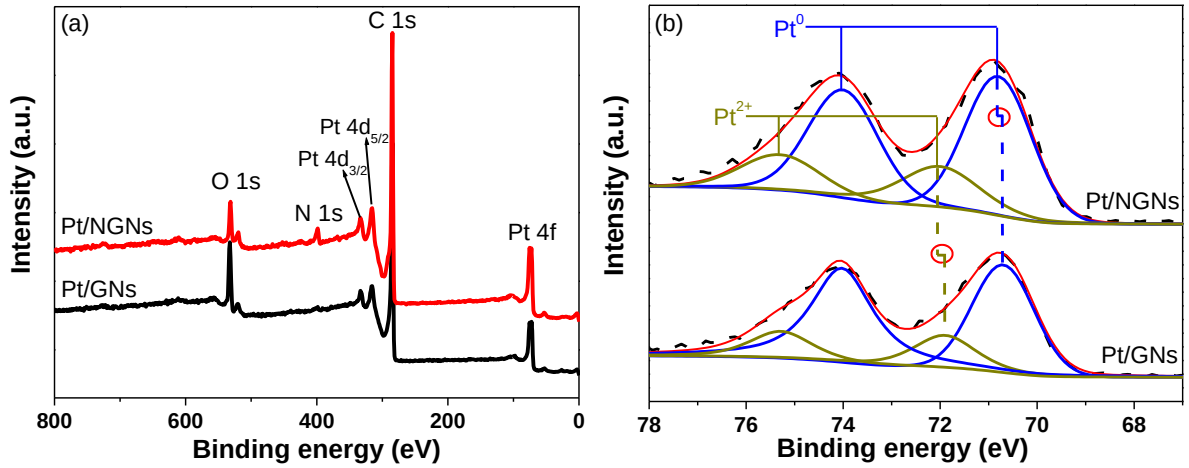

Figure 6. (a) Full XPS spectra and (b) XPS spectra in the Pt 4f region for Pt/GNs and Pt/NGNs.

Because the Pt properties were well controlled to be similar in Pt/GNs and Pt/NGNs, the stronger interaction of Pt-NGNs than that of Pt-GNs can be attributed to the N doping into GNs. As the Raman results showed (see section 3.1), N-doping in NGNs produced higher degree of defect than GNs, which might be beneficial for increasing Pt-NGNs interaction [40-42]. Correspondingly, a stronger binding of Pt particles with NGNs produces a greater electron transfer from Pt to NGNs, resulting in fewer electrons shared by CO-like poisoning species and weaker adsorption of these species on Pt, meaning superior anti-poisoning performance of Pt/NGNs in comparison with Pt/GNs [14, 43, 44].

Finally, we want to emphasize that i-t results are not only related with poisoning of catalysts, but also intimately relevant to the state of mass transfer when there are bubbles produced in catalysts layer [45]. For example, when studying methanol oxidation on Pt in acid media, three dimensional porous structures, beneficial for CO_2 removal, would result in facile transfer of methanol onto Pt surface and produce improved i-t results [25]. In such case, effects of mass transfer together with catalysts poisoning should be simultaneously considered to understand the i-t results. For the present study, since formate and methanol oxidation were measured in alkaline media with no possibility of CO_2 formation, the i-t data in this paper can be analyzed only from the aspect of catalyst poisoning.

4. CONCLUSION

In this study, we demonstrated a prototype for precisely comparing the anti-poisoning performance (APP) of series catalysts. By combining controlled preparation and modified i-t data analysis, Pt/NGNs and Pt/GNs with similar activity for formate oxidation were compared to reveal difference in APPs either for the case of formate or methanol oxidation. These result verified the

reliability of the APP analysis method and confirmed the necessity of APP analysis for catalysts evaluation. Furthermore, this study demonstrated the highly efficient supports effects on catalysts APPs, which can shed light on future work toward rational supports engineering.

ACKNOWLEDGMENTS
This research is financially supported by the National Natural Science Foundation of China (U1304215) and Natural Science Foundation of Jiangsu Province (No. BK20160277).

References

1. L. Y. Zhang, H. Y. Liu, X. Huang, X. P. Sun, Z. Jiang, R. Schlögl, D. S. Su, *Angew. Chem. Int. Ed.*, 54 (2015) 15823.
2. S. Yang, J. Kim, Y.J. Tak, A. Soon, H. Lee, *Angew. Chem. Int. Ed*., 55 (2016) 2058.
3. W. J. Huang, X. Y. Ma, H. Wang, R. F. Feng, J. G. Zhou, P. N. Duchesne, P. Zhang, F. J. Chen, N. Han, F. P. Zhao, J. H. Zhou, W. B. Cai, Y. G. Li, *Adv. Mater*., 29 (2017) 1703057.
4. N. C. Cheng, M. N. Banis, J. Liu, A. Riese, X. Li, R. Y. Li, S. Y. Ye, S. Knights, X. L. Sun, *Adv. Mater*., 27 (2015) 277.
5. W. C. Sheng, S. Chen, E. Vescovo, Y. Shao-Horn, *J. Electrochem. Soc*., 159 (2012) B96.
6. R. Siburian, T. Kondo, J. Nakamura, *J. Phys. Chem*. C, 117 (2013) 3635.
7. D. G. Li, C. Wang, D. S. Strmcnik, D. V. Tripkovic, X. L. Sun, Y. J. Kang, M. F. Chi, J. D. Snyder, D. Vliet, Y. Tsai, V. R. Stamenkovic, S. H. Sun, N. M. Markovic, *Energy Environ. Sci*., 7 (2014) 4061.
8. X. M. Qu, L. X. You, X. C. Tian, B. W. Zhang, G. D. Mahadevan, Y. X. Jiang, S. G. Sun, *Electrochim. Acta*,182 (2015) 1078.
9. C. H. Liu, X. L. Cai, J. S. Wang, J. Liu, A. Riese, Z. D. Chen, X. L. Sun, S. D. Wang, *Int. J. Hydrogen Energy*, 41 (2016) 13476.
10. J. W. Hong, D. Kim, Y. W. Lee, M. Kim, S. W. Kang, S. W. Han, *Angew. Chem. Int. Ed.*, 51 (2011) 8876.
11. M. L. Xiao, J. B. Zhu, J. J. Ge, C. P. Liu, W. Xing, *J. Power Sources*, 281 (2015) 34.
12. K. An, S. Alayoglu, N. Musselwhite, S. Plamthottam, G. Melaet, A. E. Lindeman, G. A. Somorjai, *J. Am. Chem. Soc*.,135 (2013) 16689.
13. A. S. Bandarenka, M. T. M Koper, *J. Catal.*, 308 (2013) 11.
14. Y. R. Sun, C. Du, M. C. An, L. Du, Q. Tan, C. T. Liu, Y. Z. Gao, G. P. Yin, *J. Power Sources*, 300 (2015) 245.
15. J. M. Lu, Y. K. Zhou, X. H. Tian, X. Xu, H. X. Zhu, S. W. Zhang, T. Yuan, *Appl. Surf. Sci*., 317 (2014) 284.
16. X. L. Sui, Z. B. Wang, M. Yang, L. Huo, D. M. Gu, G. P. Yin, *J. Power Sources*, 255 (2014) 43.
17. K. Jiang, J. F. Chang, H. Wang, S. Brimaud, W. Xing, R. J. Behm, W. B. Cai, *ACS Appl. Mater. Interfaces*, 8 (2016) 7133.
18. A. M. Bartrom, J. L. Haan, *J. Power Sources*, 214 (2012) 68.
19. T. Yajima, H. Uchida, M. Watanabe, *J. Phys. Chem*. B,108 (2004) 2654.
20. L.G. Feng, J. F. Chang, K. Jiang, H. G. Xue, C. P. Liu, W. B. Cai, W. Xing, J. J. Zhang, *Nano Energy*, 3 0(2016) 355.
21. P. Hernandez-Fernandez, P. B. Lund, C. Kallesøe, H. F. Clausen, L. H. Christensen, *Int. J. Hydrogen Energy*, 40 (2015) 284.
22. C. Busó-Rogero, E. Herrero, J. M. Feliu, *ChemPhysChem*, 15 (2014) 2019.
23. J. H. Jiang, J. Scott, A. Wiechowski, *Electrochim. Acta*, 104 (2013) 124.

24. J. S. Wang, C. H. Liu, B. W. Xiao, N. C. Cheng, A. Riese, M. N. Banis, X. L. Sun, *ChemElectroChem*,4 (2017) 296.
25. H. J. Huang, S. B. Yang, R. Vajtai, X. Wang, P. M. Ajayan, *Adv. Mater*., 26 (2014) 5160.
26. L. Tao, S. Dou, Z. L. Ma, A. L. Shen, S. Y. Wang, *Int. J. Hydrogen Energy*, 40 (2015) 14371.
27. E. Yoo, T. Okata, T. Akita, M. Kohyama, J. Nakamura, I. Honma, *Nano Lett*., 9 (2009) 2255.
28. A. M. Hofstead-Duffy, D. J. Chen, S. G. Sun, Y. Y. J. Tong, *J. Mater. Chem*., 22 (2012) 5205.
29. D. Y. Chung, K. J. Le, Y. E. Sung, *J. Phys. Chem*. C,120 (2016) 9028.
30. Y. Z. Zhao, X. M. Li, J. M. Schechter, Y. A. Yang, *RSC Adv*., 6 (2016) 5384.
31. J. H. Ma, L. Wang, X. Mu, L. Li, *Int. J. Hydrogen Energy*, 40 (2015) 2641.
32. C. T. Hsieh, J. L. Gu, D. Y. Tzou, Y. C. Chu, Y. C. Chen, *Int. J. Hydrogen Energy*, 38 (2013) 10345.
33. J. Noborikawa, J. Lau, J. Ta, S. Z. Hu, L. Scudiero, S. Derakhshan, S. Ha, J. L. Haan, *Electrochim. Acta*, 137 (2014) 654.
34. M. H. Seo, S. M. Choi, E. J. Lim, I. H. Kwon, J. K. Seo, S. H. Noh, W. B. Kim, B. C. Han, *ChemSusChem*, 7 (2014) 2609.
35. B. Xiong, Y. K. Zhou, Y. Y. Zhao, J. Wang, X. Chen, R. O'Hayre, Z. P. Shao, *Carbon*, 52 (2013) 181.
36. S. Y. Wang, F. Yang, S. P. Jiang, S. L. Chen, X. Wang, *Electrochem. Commun*., 12 (2010) 1646.
37. J. S. Wang, C. H. Liu, M. N. Banis, N. C. Cheng, A. Riese, S. D. Wang, X. L. Sun, *Int. J. Hydrogen Energy*, 41 (2016) 936.
38. S. Stambula, N. Gauquelin, M. Bugnet, S. Gorantla, S. Turner, S. H. Sun, J. Liu, G. X. Zhang, X. L. Sun, G. A. Botton, *J. Phys. Chem*. C, 118 (2014) 3890.
39. L. Xin, F. Yang, S. Rasouli, Y. Qiu, Z. F. Li, A. Uzunoglu, C. J. Sun, Y. Z. Liu, P. Ferreira, W. Z. Li, Y. Ren, L. A. Stanciu, J. Xie, *ACS Catal*., 6 (2016) 2642.
40. J.B. Zhu, M. L. Xiao, X. Zhao, K. Li, C. P. Liu, W. Xing, *Chem. Commun*., 50 (2014) 12201.
41. G. Kim, S. H. Jhi, *ACS Nano*., 5 (2011) 805.
42. G. F. Long, X. H. Li, K. Wan, Z. X. Liang, J. H. Piao, P. Taiakaras, *Appl. Catal. B: Environ*., 203 (2017) 541.
43. I. Fampiou, A. Ramasubramaniam, *J. Phys. Chem*. C,116 (2012) 6543.
44. J. W. Ma, A. Habrioux, C. Morais, A. Lewera, W. Vogel, Y. Verde-Gómez, G. Ramos-sanchez, P. B. Balbuena, N. Alonso-Vante, *ACS Catal*., 3 (2013) 1940.
45. J. S. Wang, X. Guo, C. Y. Song, L. C. Wang, J. H. Zhao, X. P. Qiu, *Acta Phys. Chim. Sin*., 25 (2009) 767.